CORA

Cork Open Research Archive
Cartlann Taighde Oscailte Chorcaí

Title	Conformational states of HIV-1 reverse transcriptase for nucleotide incorporation vs. pyrophosphorolysis – binding of foscarnet
Author(s)	Das, Kalyan; Balzarini, Jan; Miller, Matthew T.; Maguire, Anita R.; DeStefano, Jeffrey J.; Arnold, Eddy
Publication date	2016-05-18
Original citation	DAS, K., BALZARINI, J., MILLER, M. T., MAGUIRE, A. R., DESTEFANO, J. J. and ARNOLD, E. (2016) 'Conformational states of HIV-1 reverse transcriptase for nucleotide incorporation vs. pyrophosphorolysis – binding of foscarnet', ACS Chemical Biology, 11(8), pp. 2158-2164. doi:10.1021/acschembio.6b00187
Type of publication	Article (peer-reviewed)
Link to publisher's version	http://dx.doi.org/10.1021/acschembio.6b00187 Access to the full text of the published version may require a subscription.
Rights	**© 2016, American Chemical Society. This document is the Accepted Manuscript version of a Published Work that appeared in final form in ACS Chemical Biology, copyright © American Chemical Society, after peer review and technical editing by the publisher. To access the final edited and published work see http://pubs.acs.org/doi/abs/10.1021/acschembio.6b00187**
Embargo information	Access to this article is restricted until 12 months after publication by request of the publisher.
Embargo lift date	2017-05-18
Item downloaded from	http://hdl.handle.net/10468/3253

Downloaded on 2018-08-23T18:41:23Z

UCC

University College Cork, Ireland
Coláiste na hOllscoile Corcaigh

Conformational states of HIV-1 reverse transcriptase for nucleotide incorporation vs. pyrophosphorolysis – binding of foscarnet

Kalyan Das,[1] Jan Balzarini,[2] Matthew T. Miller,[1] Anita R. Maguire,[3] Jeffrey J. DeStefano,[4] Eddy Arnold[1,*]

[1]Center for Advanced Biotechnology and Medicine (CABM), Department of Chemistry and Chemical Biology, Rutgers University, Piscataway, New Jersey; [2]Rega Institute for Medical Research and Department of Microbiology and Immunology, KU Leuven, B-3000 Leuven, Belgium; [3]Department of Chemistry and School of Pharmacy, Analytical and Biological Chemistry Research Facility, Synthesis and Solid State Pharmaceutical Centre, University College Cork, Cork; [4]Department of Cell Biology and Molecular Genetics, University of Maryland College Park, College Park, Maryland.

*Correspondence to: Eddy Arnold, Center for Advanced Biotechnology and Medicine, 679 Hoes Lane West, Piscataway, NJ 08854. E-mail: arnold@cabm.rutgers.edu

ABSTRACT: HIV-1 reverse transcriptase (RT) catalytically incorporates individual nucleotides into a viral DNA strand complementing an RNA or DNA template strand; the polymerase active site of RT adopts multiple conformational and structural states while performing this task. The states associated are dNTP binding at the N site, catalytic incorporation of a nucleotide, release of a pyrophosphate, and translocation of the primer 3′-end to the P site. Structural characterization of each of these states may help in understanding the molecular mechanisms of drug activity and resistance, and in developing new RT inhibitors. Using a 38-mer DNA template-primer aptamer as the substrate mimic, we crystallized an RT/dsDNA complex that is catalytically active, yet translocation-incompetent in crystals. The ability of RT to perform dNTP binding and incorporation in crystals permitted obtaining a series of structures – (I) RT/DNA (P-site), (II) RT/DNA/AZTTP ternary, (III) RT/AZT-terminated DNA (N-site), and (IV) RT/AZT-terminated DNA (N-site)/foscarnet complexes. The stable N-site complex permitted binding of foscarnet as a pyrophosphate mimic. The Mg^{2+} ions dissociated after catalytic addition of AZTMP in the pre-translocated structure III, whereas ions A and B had reentered the active site to bind foscarnet in structure IV. The binding of foscarnet involves chelation with the Mg^{2+}(B) ion and interactions with K65 and R72. Analysis of interactions of foscarnet and the recently discovered nucleotide-competing RT inhibitor (NcRTI) α-T-CNP in two different conformational states of the enzyme provide insights for developing new classes of polymerase active site RT inhibitors.

INTRODUCTION

HIV-1, being a lentivirus, encodes the enzyme reverse transcriptase (RT) for copying the viral RNA into a viral dsDNA[1]. The DNA is integrated into the host cell chromosome by integrase, another viral enzyme. The DNA polymerization activity of RT is currently targeted by two classes of drugs that inhibit the enzyme by two distinct mechanisms. Non-nucleoside RT inhibitors (NNRTIs) bind to a hydrophobic pocket adjacent to the polymerase active site of RT[2,3], and an NNRTI functions as an allosteric inhibitor by perturbing the conformational state of an RT/nucleic acid complex[4-7]. In contrast, a nucleoside analog RT inhibitor (NRTI) binds as dNTP mimic, and is catalytically incorporated into the primer DNA strand by RT. All NRTIs act as DNA chain terminators because they lack a 3′-OH preventing the incorporation of next nucleotide.

Currently, five NNRTIs and eight NRTIs are approved anti-AIDS drugs. RT-inhibiting drugs are widely used in combinations with protease, integrase, and viral entry inhibitors for treating HIV-

1 infections. Like other types of HIV drugs, the effectiveness of an RT inhibitor is compromised by side effects and emergence of drug resistance upon long-term use. Various RT mutations emerge to confer resistance to NRTIs and NNRTIs[8-10]. RT confers NRTI resistance primarily (i) by exclusion or discrimination of an NRTI triphosphate from a dNTP (M184V/I and K65R are examples of exclusion mutations) and (ii) by excision, which removes an incorporated NRTI from the primer terminus by pyrophosphorolysis. The AZT (1-[(2*R*,4*S*,5*S*)-4-azido-5-(hydroxymethyl) oxolan-2-yl]-5-methylpyrimidine-2,4-dione) resistance mutations [D67N, K70R, L210W, T215Y/F and K219Q/E[11], also known as AZTr, excision-enhancing mutations (EEMs), or thymine analog mutations (TAMs)] facilitate binding of an ATP molecule to RT as a pyrophosphate donor for excision[12-14].

Periodically, new drugs are needed in the pool of available drugs for improving the treatment options for patients facing adverse side effects or resistance challenges to current drugs. Effective (i) nucleotide-competing RT inhibitors (NcRTIs) that compete with dNTP binding[15,16], or (ii) pyrophosphate mimics that would prevent pyrophosphorolysis/excision have potential for being developed as new classes of RT-inhibiting drugs. Foscarnet (phosphonoformic acid, PFA), a pyrophosphate mimic, is used to treat cytomegalovirus (CMV) eye infection in patients with AIDS. PFA is also used to treat herpes simplex virus (HSV) infections of the skin and mucous membranes in immunocompromised persons[17,18] when they do not respond to other therapies. HIV-1 RT, like other DNA polymerases, is inhibited by PFA at an IC_{50} in the sub-micromolar range[19]. PFA retains its potency against HIV-1 RT carrying NRTI and NNRTI resistance mutations[20,21]. PFA is not, however, routinely used clinically to treat HIV infection, likely due to a modest inhibitory effect. Optimization and elaboration of the PFA scaffold may help in developing more potent RT-specific drugs for treating HIV-1 infection.

Based on biochemical studies[22-24] and a crystal structure of PFA in complex with an engineered chimeric DNA polymerase (UL54) of CMV[25], PFA is expected to bind HIV-1 RT mimicking the β, γ−pyrophosphate moiety of a dNTP. Our earlier attempts to obtain a crystal structure of an RT/DNA/PFA complex were not successful using either cross-linked or non-cross-linked RT/DNA N-site complexes[14,26]. A primary challenge was to stabilize an N-site RT/nucleic acid binary complex to which PFA is expected to bind[24].
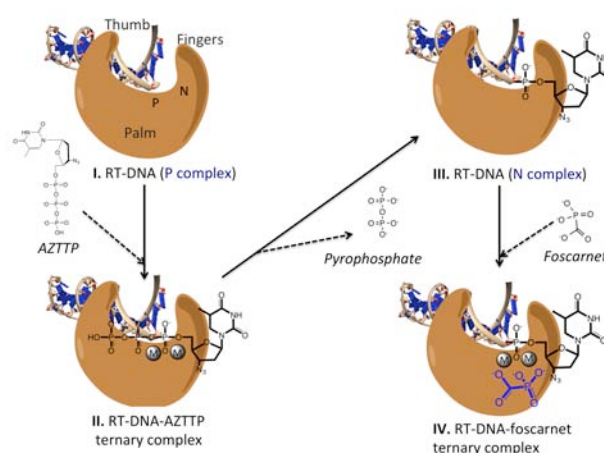

Figure 1. Structural states of HIV-1 RT trapped in crystals of RT/apt-DNA. The crystals of an RT/apt-DNA complex (**I**) were soaked with AZTTP and $CaCl_2$ for the formation of an RT/apt-DNA/AZTTP complex (**II**); N and P sites are indicated in **I**. Crystals of **I** were soaked with AZTTP and $MgCl_2$ for catalytic addition of AZTMP resulting in complex **III**. Crystals of **III** were further soaked with PFA and $MgCl_2$ for the formation of the RT/apt-DNA/PFA complex (**IV**).

Using a modified SELEX (selective evolution of ligands by exponential enrichment) approach, template-primer sequences that bind HIV-1 RT with high affinity were selected[27]. Further modification of these sequences led to the construction of a 38-mer hairpin DNA aptamer (apt-DNA) that bound HIV-1 RT with very high affinity[28]. This aptamer binds RT as a 15 base-pair duplex extending from the polymerase active site towards the RNase H domain, a three-deoxythymidine hairpin loop proximal to the RNase H domain, and a five-nucleotide 5'-overhang[29]. Here we demonstrate that the RT/apt-DNA complex is catalytically active,

permitting the binding of AZTTP as a dNTP analog and subsequently incorporating AZTMP at the 3′-end (**Figure 1**) in crystals. However, translocation of the DNA was restricted by the aptamer hairpin that is locked against the RNase H domain of RT, and this stable N-site complex in crystals permitted the binding of PFA as a pyrophosphate mimic. The RT/apt-DNA P-site complex permitted the binding of α-T-CNP[16] by coordinating with both catalytic metal ions. The binding of α-T-CNP and PFA to RT reveals two distinct conformations of the polymerase active site with different chelating environments for designing novel RT inhibitors.

RESULTS AND DISCUSSION

AZTTP binding and incorporation into apt-DNA by RT in crystals. The structure of the RT/apt-DNA complex (**I**) was recently reported at 2.3 Å resolution, revealing that the binding mode of the aptamer is similar to that of previously reported cross-linked RT/DNA complexes at and near the polymerase active site[29]. RT/DNA cross-linking were performed in conjunction with catalytic addition of one dideoxynucleotide at the primer 3′-end[30,31]. In fact, most reported DNA polymerase pre-catalytic complex structures have been determined with 3'-dideoxy-terminated nucleic acid. In contrast, the complex **I** has a 3′-OH group that is positioned at the polymerase active site for binding and catalytic addition of the next nucleotide, which is a dTTP or related analog. Ca^{2+} ions are not efficient cations for DNA polymerization by RT. We soaked AZTTP and $CaCl_2$ into crystals of **I** for the formation of a ternary complex without incorporation. As described in the experimental section, a short (5-minute) soak formed a ternary RT/DNA/AZTTP (**II**) complex in the crystal, and the structure of the complex was determined at 3.3 Å resolution (SI **Table 1**). The AZTTP binds at the N site in a mode that is analogous to the previously obtained mode of binding in RT/dsDNA/AZTTP (or dTTP) complex structures (**Figures 2A & B**)[6,30]. A Ca^{2+} ion is present at the metal B site and chelates one oxygen from each of the three phosphates of AZTTP; no ion is present at the A site. Even though the 3′-end of apt-DNA had an OH group present for incorporation of the incoming AZTMP, the use of Ca^{2+} ions was not efficient for carrying out the catalysis in the crystal within the 5-minute soaking time.
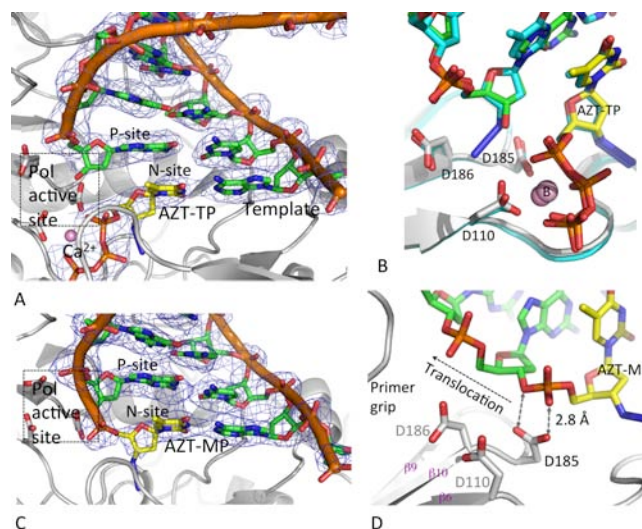

Fig. 2. Binding and incorporation of AZT-TP by RT in crystals. A. AZTTP (yellow) is bound at the polymerase active site in RT/apt-DNA/AZTTP complex (II). **B.** The ternary structures of RT/apt-DNA/AZTTP and RT/DNA/AZTTP (PDB ID. 3V4I; cyan) are highly superimposable at the polymerase active site. **C.** The polymerase active site region after incorporation of AZTMP in the RT/apt-DNA (AZTMP terminated) N-site structure (III). **D**. Location of incorporated AZTMP with respect to the catalytic triad of aspartates.

Soaking a crystal in 2.8 mM AZTTP with 25 mM $MgCl_2$ for 10 minutes, however, confirmed our hypothesis that the RT/apt-DNA complex is indeed catalytically active by incorporating an AZTMP at the 3′-end of the apt-DNA (**Figures 2C & D**). Serendipitously, the incorporated AZTMP does not translocate from the N site to the P site because the DNA hairpin is locked against the RNase H domain of RT at the opposite end, preventing the sliding of DNA in the crystal. The crystal packing analysis (**SI Figure 1**) did not indicate any noticeable interaction of apt-DNA with symmetry related molecules. Unlike a typical RT/DNA complex, which can be highly dynamic in solution[32], the RT/apt-DNA apparently forms a stable complex with enhanced protein-nucleic acid interactions. The RT/apt-

DNA-AZTMP (**III**) structure represents a state of RT/DNA complex following catalytic incorporation of a dNTP that precedes translocation. In this pre-translocation N-site state (**III**), the Mg^{2+} ions are dissociated from the polymerase active site after the catalytic addition of AZTMP, and two catalytic aspartates D110 and D186 are pointing away from nucleic acid at the active site. The phosphate oxygens of the newly formed phosphodiester bond are in close proximity to both carboxyl oxygens of the third catalytic aspartate D185 (**Figure 2D**). In a typical RT/nucleic acid complex, this congregation of negatively charged groups would either (i) repel to facilitate the nucleic acid translocation or (ii) attract cations to stabilize the N state and facilitate pyrophosphorolysis, as discussed below.

PFA binding to the RT/apt-DNA complex. PFA as a pyrophosphate mimic is expected to bind and stabilize an N-site complex[22,23]. Complex **III** in the crystal was used to obtain the structure of the RT/DNA/PFA (**IV**) complex. We soaked crystals of complex **III** in a solution containing 5 mM PFA and 25 mM $MgCl_2$ for 10 minutes to enable formation of the RT/DNA/PFA ternary complex **IV** (SI **Table 1**). Compared to complex **III,** in which the catalytic ions were dissociated from the polymerase active site, the binding of PFA importantly recruited both catalytic Mg^{2+} ions A and B to the polymerase active site in **IV** (**Figures 3A & B**). One oxygen each from the phosphate and carboxyl groups of PFA chelate metal B. Chelation of the phosphate of AZTMP, the main-chain carbonyl oxygen of V111, and one side-chain oxygen each from the catalytic residues D110 and D185 complete the octahedral coordination for metal B. Apart from the metal ion chelation, the conformation of RT did not undergo any significant alteration in changing from **III** to **IV** upon PFA binding. In comparison to the binding of a dNTP, the phosphate and the carboxyl oxygens of PFA approximately substitute for the chelating oxygens of β,γ-pyrophosphate, respectively; however, the positions of the chelating atoms are not superimposable (**Figure 3C**). The mode of chelation of PFA to RT is switched when compared with that

observed in the structure of engineered chimeric DNA polymerase UL54 complex (**Figures 3D & E**)[25]. This preferred orientation of PFA in the RT complex is apparently steered by a network of interactions of the phosphate group with RT beyond the metal interaction site. The interactions are (i) with the main-chain amide group of D113, adjacent to the polymerase active site and (ii) a salt bridge between the two non-chelating oxygens of the phosphate group of PFA and the guanidinium group of R72 (**Figure 3F**); R72 is a highly conserved amino acid residue that is essential for polymerization[33]. Additionally, the side chain of K65 interacts with the non-chelating oxygen of the carboxyl group of PFA. PFA has been reported to facilitate the removal of AZTMP from the 3′-end of the DNA primer[34]. Positioning of the phosphate group of PFA near the phosphodiester bond of incorporated AZTMP in complex **III** may facilitate the excision only when the phosphate group of PFA is oriented in-line as an excision agent. However, the PFA orientation in **III** is not appropriate to initiate excision despite the close proximity of the phosphate group to the phosphodiester bond (**Figure 3C**).
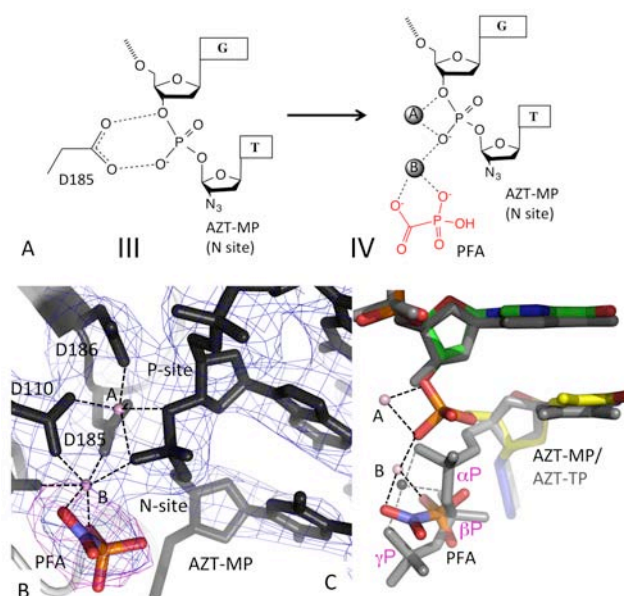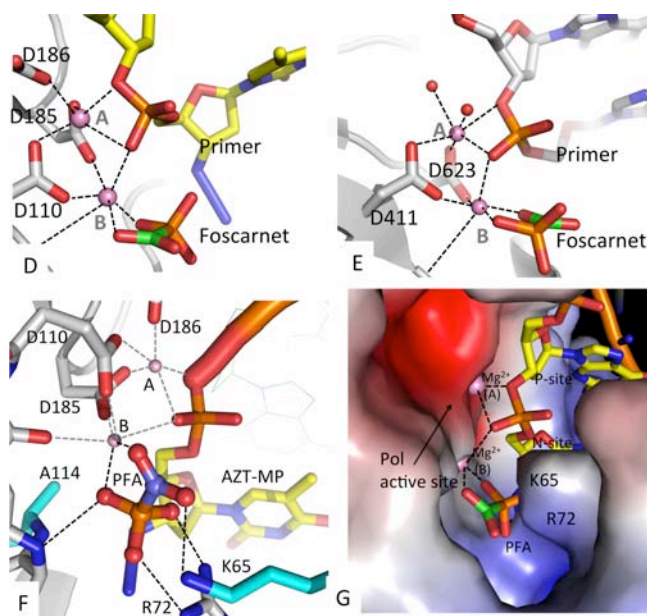
Figure 3. Binding of PFA. A. A schematic view of transition at the polymerase active site upon binding of PFA (from complex **III** to **IV**). **B.** Difference Fo - Fc (magenta) and 2Fo - Fc (blue) electron density maps at 3 Å resolution revealed the PFA binding mode and polymerase active-site conformation. **C.** Superposition of structures **II** and **IV** shows the positional differences of chelating oxygen atoms of PFA compared to the pyrophosphate moiety (β and γ phosphates) of AZTTP. Comparison of the binding modes of PFA with HIV-1 RT (**D**) and with engineered chimeric DNA polymerase UL54D[25] (**E**). **F.** Interactions of PFA with RT. The sites of PFA-resistance mutations K65R and A114S are in cyan. **G.** Electrostatic potential surface of RT and location of PFA in the complex.

PFA resistance. Commonly observed RT mutations associated with PFA resistance are K65R, W88G/S, E89K, A114S, S117T, Q161L, M164I, and Q161L/H208Y[22,35-37]. Residue K65 interacts with PFA in structure **IV**. The K65R mutation influences the positioning of amino acids R65 and R72[38], and this structural rearrangement would interfere with the observed interactions of the two amino acid residues K65/R72 with PFA (**Figures 3F & G**). Residue A114 is positioned adjacent to the phosphate group of PFA or the β−phosphate group of a dNTP substrate, and the side chain of S114 in an A114S mutant RT would perturb the position and/or charge distribution of the phosphate group. The remaining RT mutations are located away from PFA, and would interfere indirectly with PFA binding presumably by reducing the stability of the N-site complex or

by interfering with the positioning of the two metal ions. The amino acid residue stretch 88–95 interacts with the template strand adjacent to the polymerase active-site, and mutations in this stretch affect fidelity of RT[39]. Mutations at positions 88 and 89 are likely to perturb the positioning of the template strand.

Most of the PFA-resistance mutations reduce the pyrophosphorolysis by RT, *i.e*., the mutations either directly interfere with the binding of pyrophosphate or indirectly reduce the stability of an N-site RT complex. Thereby, the PFA-resistance mutations reduce the ability of RT to excise AZTMP and, consequently, improve AZT sensitivity even in the presence of AZT-resistance mutations (EEMs). Structurally, it has been shown that the EEMs primarily enhance the binding affinity of ATP as a pyrophosphate donor. As expected, comparison of the complex **IV** with the structure of the RT/DNA/AZTppppA excision product complex[14] shows that PFA would interfere with the binding/positioning of the pyrophosphate moiety of an ATP. In such a scenario, the pyrophosphate moiety would not be able to reach the active site even if EEMs enhance the binding of the base-ribose moiety of ATP to RT.

Binding of α-T-CNP. Unlike PFA, the NcRTI α-CNP binds as a dNTP mimic at the N site. There are important differences, however, in the interactions and chelation geometry for α-T-CNP compared to dTTP (or AZTTP). Recently, we reported the structure of α-T-CNP in complex with a cross-linked RT/DNA[16], in which cation A was not present at the polymerase active site primarily due to the use of a dideoxy-terminated primer. The structure of the RT/apt-DNA/α-T-CNP complex (**V**) determined at 2.75 Å resolution (**SI Table1**), however, confirm the presence of both metal ions at the polymerase active site and reveals the complete coordination of the inhibitor (**Figure 4A**).
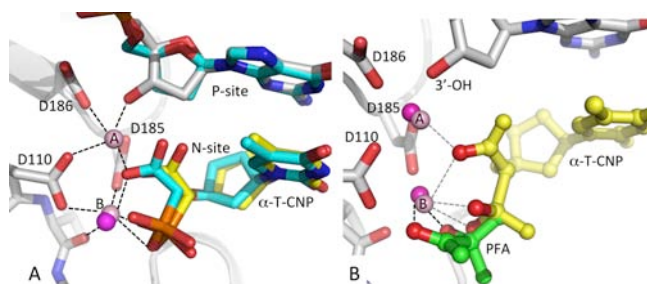
Figure 4. Binding of α-T-CNP and PFA to RT. A. Superposition of α-T-CNP (cyan) in the RT/DNA cross-linked complex (PDB Id. 4R5P)[16] on to the RT/apt-DNA/α-T-CNP complex (inhibitor, yellow; protein, gray). The current structure reveals coordination of α-T-CNP with both Mg^{2+} ions. **B.** Active site superposition of structures **IV** and **V** shows the relative positioning and metal chelation of PFA (green) and α-T-CNP (yellow); only the chelating oxygen atoms are colored red.

The structures **IV** and **V**, both being in one crystal form, provide a direct comparison of the binding of α-T-CNP and PFA to RT (**Figure 4B**); the first one as a dNTP- and the second one as a pyrophosphate-competing inhibitor, respectively. PFA binds only when the primer terminus is at the N site, and α-T-CNP binds only when the primer terminus is at the P site, *i.e.*, binding of the two inhibitors is mutually exclusive. However, each of the two inhibitors is expected to complement AZT in inhibiting RT because either one can bind when AZT is a chain terminator. AZT and PFA have earlier been demonstrated to act synergistically against HIV in cell culture[19,40,,41] and AZTTP has also been claimed to synergistically inhibit HIV-1 RT when combined with PFA[41], but only at their IC_{90} or IC_{95} concentrations, whereas antagonistically or additively inhibiting the enzyme when combined at IC_{50} or IC_{75} concentrations, respectively. These observations demonstrate the complexity of drug combinations[42], and also revealed a mutually exclusive inhibition of HIV-1 RT by AZTTP and PFA. Potential antiviral synergy between AZT (or PFA) and α-CNPs could not be tested since the current α-CNPs are not efficiently taken up by HIV-infected cells. Therefore, combinations of AZTTP with PFA, AZTTP with T-α-CNP, and PFA with T-α-CNP have been investigated for their inhibition of RT activity over a broad range of inhibitor concentrations (**SI Figure 2**). No

dramatic differences were observed in the degree of increased potencies of the anti-HIV-1 RT activity when any of the inhibitors was combined with one of the other inhibitors. The combination index (CI) *versus* fractional inhibition values, and normalized isobolograms (**SI Figure 3**) for the three different inhibitor combinations revealed additive to modest synergistic activities in all three cases, with somewhat lesser effect for the PFA/T-α-CNP combination. It should, however, be noticed that the RT assays were conducted in a cell-free system under artificial conditions. These results may reflect the dynamic states of an RT/DNA complex in solution that did not permit trapping the RT/DNA/PFA complex when the special apt-DNA was not used in the assay. Improved inhibitors with higher binding affinity may form more stable complexes.

Drug design. The active-site region of an enzyme in general is less susceptible to mutation, and therefore represents a highly valuable target for drug discovery. Information on the precise metal chelation geometry[43] and the surrounding environment can help in designing target-specific inhibitors. Derivatives of 4-chlorophenyl hydrazine mesoxalic acid (CPHM) have been identified as translocation inhibitors[44,45]. Analogous to PFA, CPHM compounds are predicted to preferentially bind to N-site complexes of RT. Despite both inhibitors chelating the polymerase active site cations, the interactions of the distinct side groups with RT define their respective binding affinity and impacts of resistance mutations; K65R mutation favors CPHM binding and develops resistance to PFA. K65R mutation forms a guanidinium platform with R72[38], and the platform presumably stacks favorably with the aromatic side group of CPHM. The malonate group of CPHM might chelate Mg^{2+} ions of an N complex in a mode analogous to the structurally observed mode of chelation of a malonate-containing NcRTI to the P complex (PDB ID 5HLF)[46]. In the context of antiviral activity, PFA inhibits HIV, whereas, the malonate-containing NcRTI and CPHM fail to exhibit antiviral response presumably because of their inability to penetrate the cell wall. The comparison of PFA

and CPHM in inhibiting RT suggests that chemical modifications of the compounds binding to the N or P complex could be exploited for improved RT binding and cellular uptake.

Additionally, the individual conformational states of the active site of RT can ideally be targeted and trapped by small molecules. Active-site metal-chelating inhibitors, such as the HIV-1 integrase-inhibiting drugs raltegravir, elvitegravir, and dolutegravir, chelate the catalytic metal ions of the intasome complex to block strand transfer[47,48]. A systematic elaboration from the metal-chelating diketo acid moiety helped gain specificity and efficacy even in the absence of any three-dimensional structural information[47]. In an analogous platform, knowledge of the binding and chelation of PFA or α-T-CNP at the polymerase active site of RT provides opportunities for developing new RT-inhibiting drugs. In agreement with the existing biochemical data, the structural data show that PFA binding stabilizes the N-site complex, and PFA binding would inhibit pyrophosphorolysis as a pyrophosphate-competing inhibitor. Mutations that would reduce the binding of PFA are likely to reduce the binding of a pyrophosphate donor and excision. Therefore, either the presence of PFA or PFA-resistance mutations, in general, suppresses AZT resistance both in viral and enzymatic studies[37,49]. RT has to compromise its activity for developing resistance to PFA, however, the binding affinity of PFA to RT is modest due to the lack of RT-specific interactions. The structure of **IV** reveals the conformational state of RT and the molecular interactions between RT and PFA. Chemical elaboration of the PFA backbone aided by knowledge of the structure may lead to improved pyrophosphate-mimicking inhibitors. Combining structural features of α-T-CNP/AZTTP at the N-site and PFA (**Figure 4B**) may help to develop novel high-affinity NcRTIs that can exhibit antiviral activity.

CONCLUSIONS

A special 38-mer DNA aptamer permitted obtaining the crystal structure of a highly stable HIV-1 RT/DNA complex (**I**)[29], and the crystals were used to obtain the structures with bound AZTTP (**II**), AZT-MP incorporated at the N site (**III**), and PFA bound to an N-site complex (**IV**) (**Figure 1**). Also, a structure of the NcRTI, α-T-CNP (**V**), chelating both catalytic Mg^{2+} ions at the polymerase active site of RT, is reported here for the first time. This series of structures illuminate multiple conformational states of the polymerase site that HIV-1 RT would undertake for processing nucleotide addition or pyrophosphorolysis. The structural knowledge of these distinct states of the active site may enhance understanding the molecular mechanisms of various drug-resistance mutations and help in targeting DNA polymerization by new classes of active-site-chelating inhibitors.

MATERIALS AND METHODS

Reverse transcriptase assay with homopolymeric template-primers. HIV-I RT assays were carried out in the presence of the artificial homopolymeric template-primer poly(A)•dT$_{12\text{-}18}$ (oligo(dT), Pharmacia, Uppsala, Sweden). To prepare the template-primer for the RT inhibition experiments, 0.15 mM poly(A) was mixed with an equal volume of 0.0375 mM oligo(dT). The reaction mixture (50 μl) contained 50 mM Tris•HC1 pH 7.8, 5 mM dithiothreitol, 300 mM glutathione, 500 μM EDTA, 150 mM KCl, 5 mM $MgCl_2$, 1.25 μg of bovine serum albumin, an appropriate concentration of the tritium-labeled substrate [CH$_3$-^{3}H]dTTP (2 μCi/assay; 2 μM), a fixed concentration of the template-primer poly(A).oligo(dT) (0.015 mM), 0.06% Triton X-100, 10 μl of AZTTP, T-α-CNP and/or PFA inhibitor solution (containing various concentrations of the compounds or dual combinations thereof), and 1 μl of the HIV-1 RT preparation. The reaction mixtures were incubated at 37 °C for 30 minutes, at which time 100 μl of calf thymus DNA (150 μg/ml), 2 ml of $Na_4P_2O_7$ (0.1 M in 1 M HCl), and 2 ml of trichloroacetic acid (10% v/v) were added. The solutions were kept on ice for 30 minutes, after which the acid-insoluble material was washed and analyzed for radioactivity. The inhibition data were processed using

CompuSyn software. Synergism, additivity, or antagonism was determined by calculation of the combination index (CI) values. A CI<0.95 indicates synergism, >1.05 antagonism, and between 0.95 and 1.05 represents additivity according to Kong et al.[42] and Chou and Talalay[50].

Crystallography. RT purification and crystallization with apt-DNA were carried out using earlier described experimental conditions[29]. Crystals of RT/apt-DNA (**I**) complex were soaked in the crystallization solution containing 25 mM $CaCl_2$ and 2.8 mM AZTTP for 5 minutes for the formation of RT/apt-DNA/AZTTP ternary complex (**II**). Crystals of **I** were soaked with 25 mM $MgCl_2$ and 2.8 mM AZTTP for 10 minutes, and the condition was suitable for catalytic incorporation of AZTMP at the 3′-end of the apt-DNA by RT to form the RT/AZT-terminated apt-DNA N-site complex (**III**). Crystals of **III** were then soaked in a solution containing 25 mM $MgCl_2$ and 5 mM PFA for 1 hour for the formation of RT/apt-DNA/PFA ternary complex (**IV**). Crystals of **I** were soaked in a solution containing 25 mM $MgCl_2$ and 2 mM α-T-CNP for the formation of RT/apt-DNA/α-T-CNP ternary complex (**V**). All crystal soaking solutions contained 10% (w/v) PEG 8000, 25 mM Bis-tris propane pH 6.8, 75 mM Bis-tris propane pH 7.4, 50 mM ammonium sulfate, 5% (v/v) glycerol, and 5% (w/v) sucrose. The cryoprotectant solutions in which the crystals were dipped prior to flash cooling were made from the respective soaking solution by increasing the glycerol concentration to 25% (v/v). X-ray diffraction data were collected using synchrotron beam lines; the initial structures were solved using the structure of RT/apt-DNA complex (PDB ID 5D3G) as the starting model. The structures were refined using Phenix[51] and the model building was carried out using Coot[52]. The crystallographic data and refinement statistics are listed in SI Table 1, and the coordinates and structure factors were deposited in the PDB under accession codes 5I42, 5I3U, 5HP1, and 5HRO for structures **II** to **V**, respectively.

ASSOCIATED CONTENT

AUTHOR INFORMATION

Corresponding Author

*Correspondence to: Eddy Arnold, Center for Advanced Biotechnology and Medicine, 679 Hoes Lane West, Piscataway, NJ 08854. E-mail: arnold@cabm.rutgers.edu

Notes

Any additional relevant notes should be placed here.

ACKNOWLEDGMENTS

ABBREVIATIONS

Apt-DNA, 38-mer aptamer DNA; CMV, cytomegalovirus; dsDNA, double-stranded DNA; EEM, excision-enhancing mutation; NcRTI, nucleotide-competing RT inhibitor; NNRTI, non-nucleoside RT inhibitor; NRTI, nucleoside RT inhibitor; PFA, phosphonoformic acid; TAM, thymine analog mutation.

REFERENCES

1. Hu, W. S., and Hughes, S. H. (2012) HIV-1 reverse transcription. *Cold Spring Harb Perspect Med* 2
2. Kohlstaedt, L. A., Wang, J., Friedman, J. M., Rice, P. A., and Steitz, T. A. (1992) Crystal structure at 3.5 Å resolution of HIV-1 reverse transcriptase complexed with an inhibitor. *Science* 256, 1783-1790
3. Das, K., Clark, J., A.D., , Lewi, P. J., Heeres, J., de Jonge, M. R., Koymans, L. M. H., Vinkers, H. M., Daeyaert, F., Ludovici, D. W., Kukla, M. J., De Corte, B., Kavash, R. W., Ho, C. Y., Ye, H., Lichtenstein, M. A., Andries, K., Pauwels, R., de Béthune, M.-P., Boyer, P. L., Clark, P., Hughes, S. H., Janssen, P. A. J., and Arnold, E. (2004) Roles of Conformational and Positional Adaptability in Structure-Based Design of TMC125-R165335 (Etravirine) and Related Non-nucleoside Reverse Transcriptase Inhibitors

That Are Highly Potent and Effective against Wild-Type and Drug-Resistant HIV-1 Variants. *J. Med. Chem.* 47, 2550-2560

4. Spence, R. A., Kati, W. M., Anderson, K. S., and Johnson, K. A. (1995) Mechanism of inhibition of HIV-1 reverse transcriptase by nonnucleoside inhibitors. *Science* 267, 988-993.

5. Rittinger, K., Divita, G., and Goody, R. S. (1995) Human immunodeficiency virus reverse transcriptase substrate-induced conformational changes and the mechanism of inhibition by nonnucleoside inhibitors. *Proc Natl Acad Sci U S A* 92, 8046-8049.

6. Das, K., Martinez, S. E., Bauman, J. D., and Arnold, E. (2012) HIV-1 reverse transcriptase complex with DNA and nevirapine reveals non-nucleoside inhibition mechanism. *Nat Struct Mol Biol* 19, 253-259

7. Bec, G., Meyer, B., Gerard, M. A., Steger, J., Fauster, K., Wolff, P., Burnouf, D., Micura, R., Dumas, P., and Ennifar, E. (2013) Thermodynamics of HIV-1 reverse transcriptase in action elucidates the mechanism of action of non-nucleoside inhibitors. *J Am Chem Soc* 135, 9743-9752

8. Menendez-Arias, L. (2008) Mechanisms of resistance to nucleoside analogue inhibitors of HIV-1 reverse transcriptase. *Virus Res* 134, 124-146

9. Das, K., and Arnold, E. (2013) HIV-1 reverse transcriptase and antiviral drug resistance. Part 1. *Curr Opin Virol* 3, 111-118

10. Das, K., and Arnold, E. (2013) HIV-1 reverse transcriptase and antiviral drug resistance. Part 2. *Curr Opin Virol* 3, 119-128

11. Larder, B. A., Darby, G., and Richman, D. D. (1989) HIV with reduced sensitivity to zidovudine (AZT) isolated during prolonged therapy. *Science* 243, 1731-1734

12. Arion, D., and Parniak, M. A. (1999) HIV resistance to zidovudine: the role of pyrophosphorolysis. *Drug Resist Updat* 2, 91-95

13. Meyer, P. R., Matsuura, S. E., Mian, A. M., So, A. G., and Scott, W. A. (1999) A mechanism of AZT resistance: an increase in nucleotide-dependent primer unblocking by mutant HIV-1 reverse transcriptase. *Mol Cell* 4, 35-43

14. Tu, X., Das, K., Han, Q., Bauman, J. D., Clark, A. D., Jr., Hou, X., Frenkel, Y. V., Gaffney, B. L., Jones, R. A., Boyer, P. L., Hughes, S. H., Sarafianos, S. G., and Arnold, E. (2010) Structural basis of HIV-1 resistance to AZT by excision. *Nat Struct Mol Biol* 17, 1202-1209

15. Jochmans, D., Deval, J., Kesteleyn, B., Van Marck, H., Bettens, E., De Baere, I., Dehertogh, P., Ivens, T., Van Ginderen, M., Van Schoubroeck, B., Ehteshami, M., Wigerinck, P., Gotte, M., and Hertogs, K. (2006) Indolopyridones inhibit human immunodeficiency virus reverse transcriptase with a novel mechanism of action. *J Virol* 80, 12283-12292

16. Balzarini, J., Das, K., Bernatchez, J. A., Martinez, S. E., Ngure, M., Keane, S., Ford, A., Maguire, N., Mullins, N., John, J., Kim, Y., Dehaen, W., Vande Voorde, J., Liekens, S., Naesens, L., Gotte, M., Maguire, A. R., and Arnold, E. (2015) Alpha-carboxy nucleoside phosphonates as universal nucleoside triphosphate mimics. *Proc Natl Acad Sci U S A* 112, 3475-3480

17. Eriksson, B., Oberg, B., and Wahren, B. (1982) Pyrophosphate analogues as inhibitors of DNA polymerases of cytomegalovirus, herpes simplex virus and cellular origin. *Biochim Biophys Acta* 696, 115-123

18. Wagstaff, A. J., and Bryson, H. M. (1994) Foscarnet. A reappraisal of its antiviral activity, pharmacokinetic properties and therapeutic use in immunocompromised patients with viral infections. *Drugs* 48, 199-226

19. Vrang, L., and Oberg, B. (1986) PPi analogs as inhibitors of human T-lymphotropic virus type III reverse transcriptase. *Antimicrob Agents Chemother* 29, 867-872

20. Schmit, J. C., Cogniaux, J., Hermans, P., Van Vaeck, C., Sprecher, S., Van Remoortel, B., Witvrouw, M., Balzarini, J., Desmyter, J., De Clercq, E., and Vandamme, A. M. (1996) Multiple drug resistance to nucleoside analogues and nonnucleoside reverse transcriptase inhibitors in an efficiently replicating human immunodeficiency virus type 1 patient strain. *J Infect Dis* 174, 962-968

21. Canestri, A., Ghosn, J., Wirden, M., Marguet, F., Ktorza, N., Boubezari, I., Dominguez, S., Bossi, P., Caumes, E., Calvez, V., and Katlama, C. (2006) Foscarnet salvage therapy for patients with late-stage HIV disease and multiple drug resistance. *Antiviral Therapy* 11, 561-566

22. Meyer, P. R., Matsuura, S. E., Zonarich, D., Chopra, R. R., Pendarvis, E., Bazmi, H. Z., Mellors, J. W., and Scott, W. A. (2003)

Relationship between 3'-azido-3'-deoxythymidine resistance and primer unblocking activity in foscarnet-resistant mutants of human immunodeficiency virus type 1 reverse transcriptase. *J Virol* 77, 6127-6137

23. Marchand, B., Tchesnokov, E. P., and Gotte, M. (2007) The pyrophosphate analogue foscarnet traps the pre-translocational state of HIV-1 reverse transcriptase in a Brownian ratchet model of polymerase translocation. *J Biol Chem* 282, 3337-3346

24. Beilhartz, G. L., Wendeler, M., Baichoo, N., Rausch, J., Le Grice, S., and Gotte, M. (2009) HIV-1 reverse transcriptase can simultaneously engage its DNA/RNA substrate at both DNA polymerase and RNase H active sites: implications for RNase H inhibition. *J Mol Biol* 388, 462-474

25. Zahn, K. E., Tchesnokov, E. P., Gotte, M., and Doublie, S. (2011) Phosphonoformic acid inhibits viral replication by trapping the closed form of the DNA polymerase. *J Biol Chem* 286, 25246-25255

26. Sarafianos, S. G., Clark, A. D., Jr., Das, K., Tuske, S., Birktoft, J. J., Ilankumaran, P., Ramesha, A. R., Sayer, J. M., Jerina, D. M., Boyer, P. L., Hughes, S. H., and Arnold, E. (2002) Structures of HIV-1 reverse transcriptase with pre- and post-translocation AZTMP-terminated DNA. *EMBO J* 21, 6614-6624.

27. DeStefano, J. J., and Cristofaro, J. V. (2006) Selection of primer-template sequences that bind human immunodeficiency virus reverse transcriptase with high affinity. *Nucleic Acids Res* 34, 130-139

28. DeStefano, J. J., and Nair, G. R. (2008) Novel aptamer inhibitors of human immunodeficiency virus reverse transcriptase. *Oligonucleotides* 18, 133-144

29. Miller, M. T., Tuske, S., Das, K., DeStefano, J. J., and Arnold, E. (2016) Structure of HIV-1 reverse transcriptase bound to a novel 38-mer hairpin template-primer DNA aptamer. *Protein Science* 25, 46-55

30. Huang, H., Chopra, R., Verdine, G. L., and Harrison, S. C. (1998) Structure of a covalently trapped catalytic complex of HIV-1 reverse transcriptase: implications for drug resistance. *Science* 282, 1669-1675

31. Sarafianos, S. G., Clark, A. D., Jr., Tuske, S., Squire, C. J., Das, K., Sheng, D., Ilankumaran, P., Ramesha, A. R., Kroth, H., Sayer, J. M.,

Jerina, D. M., Boyer, P. L., Hughes, S. H., and Arnold, E. (2003) Trapping HIV-1 reverse transcriptase before and after translocation on DNA. *J Biol Chem* 278, 16280-16288

32. Abbondanzieri, E. A., Bokinsky, G., Rausch, J. W., Zhang, J. X., Le Grice, S. F., and Zhuang, X. (2008) Dynamic binding orientations direct activity of HIV reverse transcriptase. *Nature* 453, 184-189

33. Sarafianos, S. G., Pandey, V. N., Kaushik, N., and Modak, M. J. (1995) Site-directed mutagenesis of arginine 72 of HIV-1 reverse transcriptase. Catalytic role and inhibitor sensitivity. *J Biol Chem* 270, 19729-19735

34. Cruchaga, C., Anso, E., Rouzaut, A., and Martinez-Irujo, J. J. (2006) Selective excision of chain-terminating nucleotides by HIV-1 reverse transcriptase with phosphonoformate as substrate. *J Biol Chem* 281, 27744-27752

35. Mellors, J. W., Bazmi, H. Z., Schinazi, R. F., Roy, B. M., Hsiou, Y., Arnold, E., Weir, J., and Mayers, D. L. (1995) Novel mutations in reverse transcriptase of human immunodeficiency virus type 1 reduce susceptibility to foscarnet in laboratory and clinical isolates. *Antimicrob Agents Chemother* 39, 1087-1092

36. Tachedjian, G., Mellors, J., Bazmi, H., Birch, C., and Mills, J. (1996) Zidovudine resistance is suppressed by mutations conferring resistance of human immunodeficiency virus type 1 to foscarnet. *J Virol* 70, 7171-7181

37. Arion, D., Sluis-Cremer, N., and Parniak, M. A. (2000) Mechanism by which phosphonoformic acid resistance mutations restore 3'-azido-3'-deoxythymidine (AZT) sensitivity to AZT-resistant HIV-1 reverse transcriptase. *J Biol Chem* 275, 9251-9255

38. Das, K., Bandwar, R. P., White, K. L., Feng, J. Y., Sarafianos, S. G., Tuske, S., Tu, X., Clark, A. D., Jr., Boyer, P. L., Hou, X., Gaffney, B. L., Jones, R. A., Miller, M. D., Hughes, S. H., and Arnold, E. (2009) Structural basis for the role of the K65R mutation in HIV-1 reverse transcriptase polymerization, excision antagonism, and tenofovir resistance. *J Biol Chem* 284, 35092-35100

39. Drosopoulos, W. C., and Prasad, V. R. (1996) Increased polymerase fidelity of E89G, a nucleoside analog-resistant variant of human immunodeficiency virus type 1 reverse transcriptase. *J Virol* 70, 4834-4838

40. Koshida, R., Vrang, L., Gilljam, G., Harmenberg, J., Oberg, B., and Wahren, B. (1989) Inhibition of human immunodeficiency virus in vitro by combinations of 3'-azido-3'-deoxythymidine and foscarnet. *Antimicrob Agents Chemother* 33, 778-780

41. Kong, X. B., Zhu, Q. Y., Ruprecht, R. M., Watanabe, K. A., Zeidler, J. M., Gold, J. W., Polsky, B., Armstrong, D., and Chou, T. C. (1991) Synergistic inhibition of human immunodeficiency virus type 1 replication in vitro by two-drug and three-drug combinations of 3'-azido-3'-deoxythymidine, phosphonoformate, and 2',3'-dideoxythymidine. *Antimicrob Agents Chemother* 35, 2003-2011

42. Starnes, M. C., and Cheng, Y. C. (1989) Inhibition of human immunodeficiency virus reverse transcriptase by 2',3'-dideoxynucleoside triphosphates: template dependence, and combination with phosphonoformate. *Virus Genes* 2, 241-251

43. Palermo, G., Cavalli, A., Klein, M. L., Alfonso-Prieto, M., Dal Peraro, M., and De Vivo, M. (2015) Catalytic metal ions and enzymatic processing of DNA and RNA. *Accts Chem Res* 48, 220-228

44. Davis, W. R., Tomsho, J., Nikam, S., Cook, E. M., Somand, D., and Peliska, J. A. (2000) Inhibition of HIV-1 reverse transcriptase-catalyzed DNA strand transfer reactions by 4-chlorophenylhydrazone of mesoxalic acid. *Biochemistry* 39, 14279-14291

45. Bernatchez, J. A., Paul, R., Tchesnokov, E. P., Ngure, M., Beilhartz, G. L., Berghuis, A. M., Lavoie, R., Li, L., Auger, A., Melnyk, R. A., Grobler, J. A., Miller, M. D., Hazuda, D. J., Hecht, S. M., and Gotte, M. (2015) Derivatives of mesoxalic acid block translocation of HIV-1 reverse transcriptase. *J Biol Chem* 290, 1474-1484

46. Mullins, N. D., Maguire, N. M., Ford, A., Das, K., Arnold, E., Balzarini, J., and Maguire, A. R. (2016) Exploring the role of the alpha-carboxyphosphonate moiety in the HIV-RT activity of alpha-carboxy nucleoside phosphonates. *Org Biomol Chem* 14, 2454-2465

47. Grobler, J. A., Stillmock, K., Hu, B., Witmer, M., Felock, P., Espeseth, A. S., Wolfe, A., Egbertson, M., Bourgeois, M., Melamed, J., Wai, J. S., Young, S., Vacca, J., and Hazuda, D. J. (2002) Diketo acid inhibitor mechanism and HIV-1 integrase: implications for metal binding in the active site of phosphotransferase enzymes. *Proc Natl Acad Sci U S A* 99, 6661-6666

48. Hare, S., Gupta, S. S., Valkov, E., Engelman, A., and Cherepanov, P. (2010) Retroviral intasome assembly and inhibition of DNA strand transfer. *Nature* 464, 232-236

49. Smith, R. A., Anderson, D. J., and Preston, B. D. (2006) Hypersusceptibility to substrate analogs conferred by mutations in human immunodeficiency virus type 1 reverse transcriptase. *J Virol* 80, 7169-7178

50. Chou, T. C., and Talalay, P. (1984) Quantitative analysis of dose-effect relationships: the combined effects of multiple drugs or enzyme inhibitors. *Adv Enz Reg* 22, 27-55

51. Adams, P. D., Afonine, P. V., Bunkoczi, G., Chen, V. B., Davis, I. W., Echols, N., Headd, J. J., Hung, L. W., Kapral, G. J., Grosse-Kunstleve, R. W., McCoy, A. J., Moriarty, N. W., Oeffner, R., Read, R. J., Richardson, D. C., Richardson, J. S., Terwilliger, T. C., and Zwart, P. H. (2010) PHENIX: a comprehensive Python-based system for macromolecular structure solution. *Acta Crystallogr D* 66, 213-221

52. Emsley, P., and Cowtan, K. (2004) Coot: model-building tools for molecular graphics. *Acta Crystallogr D* 60, 2126-2132

SYNOPSIS TOC